

Title: Lung ultrasound for critically ill patients

Authors:

1. Francesco Mojoli, MD

Department of clinical-surgical, diagnostic and pediatric sciences, Unit of anaesthesia and intensive care, University of Pavia, Pavia, Italy

Anesthesia and Intensive Care, Fondazione Istituto di Ricovero e Cura a Carattere Scientifico, Policlinico San Matteo, Pavia, Italy

2. Bélaid Bouhemad, MD PhD

Dijon and Université Bourgogne Franche-Comté, LNC UMR866, F-21000 Dijon, France, BP 77908, 21709 Dijon Cedex, France

Department of Anesthesiology and Intensive Care, C.H.U. Dijon, Dijon Cedex

3. Silvia Mongodi, MD PhD

Anesthesia and Intensive Care, Fondazione Istituto di Ricovero e Cura a Carattere Scientifico, Policlinico San Matteo, Pavia, Italy

4. Daniel Lichtenstein, MD

Medical intensive care unit, Hospital Ambroise Paré, Boulogne (Paris-West university), France

Corresponding author:

Pr. Francesco Mojoli

Rianimazione I, Fondazione IRCCS Policlinico S. Matteo, Viale Golgi 19, Pavia, Italy

Mail: francesco.mojoli@unipv.it

Fax: 0039 – 0382 – 501026

Phone: 0039 – 0382 – 503477

Authors' contributions: all the authors gave substantial contribution to the conception and design of the work; all authors drafted the work and revised it critically before submission (introduction: FM, BB, SM, DL; technique and basic semiotics: FM, BB, SM, DL; a diagnostic tool for the acute patient: FM, BB, SM, DL; a monitoring tool: FM, BB, SM; lung ultrasound guided mechanical ventilation: FM, BB, SM; detection and management of respiratory complications: FM, BB, SM; limitations: FM, BB, SM, DL; conclusions: FM, BB, SM, DL; tables and figures: FM, BB, SM, DL).

Sources of support: none

Running head: Lung ultrasound: from basic signs to advanced applications

Word count: 3899

Abstract word count: 200

At a glance commentary:

Point-of-care ultrasound is increasingly used at the bedside to integrate the clinical assessment of the critically ill; in particular, lung ultrasound greatly developed in the last decade. This review describes basic lung ultrasound signs and focuses on their applications in critical care. Lung semiotic is made both of artifacts (derived by air/tissue interface) and

real images (i.e. effusions and consolidations), both providing significant information to identify the main acute respiratory disorders. Lung ultrasound signs, either alone or combined to other point-of-care ultrasound techniques, are helpful in the diagnostic approach to patients with acute respiratory failure, circulatory shock or cardiac arrest. Moreover, semi-quantification of lung aeration can be performed at the bedside and used in mechanically ventilated patients to guide PEEP setting, to assess the efficacy of treatments, to monitor the evolution of the respiratory disorder, and to help the weaning process. Finally, lung ultrasound can be used for early detection and management of respiratory complications under mechanical ventilation, such as pneumothorax, ventilator-associated pneumonia, atelectasis and pleural effusions. In conclusion, lung ultrasound is a useful diagnostic and monitoring tool that might become in the next future part of the basic knowledge of physicians taking care of the critically ill patient.

Abstract

Point-of-care ultrasound is increasingly used at the bedside to integrate the clinical assessment of the critically ill; in particular, lung ultrasound greatly developed in the last decade. This review describes basic lung ultrasound signs and focuses on their applications in critical care. Lung semiotic is made both of artifacts (derived by air/tissue interface) and real images (i.e. effusions and consolidations), both providing significant information to identify the main acute respiratory disorders. Lung ultrasound signs, either alone or combined to other point-of-care ultrasound techniques, are helpful in the diagnostic approach to patients with acute respiratory failure, circulatory shock or cardiac arrest. Moreover, a semi-quantification of lung aeration can be performed at the bedside and used in mechanically ventilated patients to guide PEEP setting, to assess the efficacy of treatments, to monitor the evolution of the respiratory disorder, and to help the weaning process. Finally, lung ultrasound can be used for early detection and management of respiratory complications under mechanical ventilation, such as pneumothorax, ventilator-associated pneumonia, atelectasis and pleural effusions.

In conclusion, lung ultrasound is a useful diagnostic and monitoring tool that might become in the next future part of the basic knowledge of physicians taking care of the critically ill patient.

Abstract word count: 200

Keywords: thoracic ultrasound; mechanical ventilation; lung monitoring; acute respiratory failure

Introduction

In recent years ultrasound has earned a leading position among imaging techniques integrating clinical and instrumental bedside assessment of the critically ill (1). Point-of-care ultrasound is now generally recognized as useful and in some cases mandatory – for instance, for procedure guidance (2). Its application at the bedside includes differential diagnosis and therapeutic management of complex clinical pictures such as hemodynamic instability (3), acute respiratory failure (4) or cardiac arrest (5). Multiple ultrasound techniques are here combined and among these lung ultrasound has developed the most in the last few years.

Although the first description of ultrasound evaluation of the lung dates back 50 years ago (6) and basic signs in lung ultrasound were systematically described in the 90s (7-10), the technique has spread mainly in the last decade and its positive impact on clinical management is now suggested (11,12). This review describes basic lung ultrasound semiotics and its applications in the critically ill, with specific focus on the mechanically ventilated patient.

The technique and basic semiotics

In the thorax air and water mingle: this explains the signs of lung ultrasound (8). Because of the difference in acoustic impedance between air in the lung and superficial tissues, ultrasound cannot penetrate the lung and artifacts are generated by the pleura. A peculiarity of lung ultrasound findings is that they are made up of both artifacts (normal and pathological) and real images (always pathological and visible only in the absence of air interposition).

Here we schematically recall the basic principles of lung ultrasound, its main signs and how they are generated; the definitions which we use correspond to the 2012 international consensus conference (13)(Figures 1-3, Table 1). A simple machine is perfectly suitable; in modern machines, harmonics and artifact-erasing software have to be **deactivated**. There is **no evidence of any one probe being better than another**: a single high-resolution microconvex probe with wide frequency range, or a combination of a linear high-frequency probe and a convex/phased-array low-frequency probe can both be used; **high and low frequency** settings **adequately assess both** the pleura and deeper findings, such as consolidations and effusions.

The lung is a broad organ and many standardizations have been proposed for exploring it: the Bedside Lung Ultrasound in Emergency (**BLUE**) protocol defines three points of interest per lung, the “BLUE-points” (4). The international consensus conference (13) suggests an **eight-region** approach for antero-lateral fields examination in the **emergency department**, while a **more comprehensive twelve-region** examination is frequently used in intensive **care unit (ICU)** (Supplementary Figure 1)(14-16).

Artifacts

Almost all acute respiratory disorders involve the pleura and are therefore accessible to lung ultrasound, which is a surface imaging technique. The **lung ultrasound artifacts** come **from the pleura** and therefore the **pleural line** must be **clearly detected to avoid mistakes**. In adults it is located 0.5 cm below the rib line (**bat sign**) and always corresponds to the **parietal pleura**, while the visceral pleura can be present or not (Figure 1A).

The **A-lines** are horizontal **hyperechoic artifacts**, being **repetition** of the **pleural line** due to

ultrasound **reverberation** between the pleura and the probe. The presence of **A-lines** indicates a **high gas-volume ratio below the parietal pleura** (Figure 1A – Video 1)(17, 18), and thus can be associated with either **normal lung, hyperinflation or pneumothorax**. Other ultrasound signs allow distinguishing these conditions.

The movement of the pleural line synchronous with tidal ventilation is called **lung sliding** and indicates that the parietal and visceral pleura are apposed, the latter sliding beneath the former (7). **M-mode** allows a more precise analysis of lung sliding and shows the **“seashore sign”** (Figure 2A). If lung **sliding is absent**, a **“lung pulse”** can often be visualized in bidimensional ultrasound and M-mode (Figure 2B): the **visceral pleura only moves with the transmitted cardiac activity and not with tidal ventilation** (19). **Anterior lung sliding and lung pulse rule out pneumothorax** and provide information about regional tidal ventilation (7,19); the **absence** of lung **sliding/lung pulse** is visualized in M-mode as the **“stratosphere sign”** (Figure 2C). The **lung point** is the alternation of normal and abolished lung sliding with exclusive A-lines and is specific for **pneumothorax**: it corresponds to the point where the collapsed lung comes in touch with the parietal wall at each inspiration (Figure 2D – Video 2) (20).

The B-lines (Figure 1B) (17) are **comet-tail artifacts** always **arising from the pleural line**, moving in **concert with lung sliding**. They are usually well defined, long, extending to the bottom of the screen, erasing A-lines and **hyperechoic**. **More than two B-lines** per scan make a B-pattern (13) – historically labelled **“lung rockets”** – which is compatible with **interstitial syndrome**. **Three or four B-lines** correlate with **thickened** subpleural **interlobular** septa; **five or more** correlate with **ground-glass** areas and indicate **severe interstitial syndrome** (8).

Real images

Fluid pleural **effusion** is usually a **hypo- or an-echoic** area bounded by parietal and visceral pleuras and rib shadows (Figure 1D, Figure 3D-F)(21,22). M-mode of the effusion shows the “sinusoid sign” (Figure 1E), a floating motion of the lung within the effusion in case of low fluid viscosity (22).

Lung **consolidation** is either **non-translobar**, giving small subpleural echo-poor images with deep irregular boundaries called “**shred sign**” (Figure 1C, video 3), or **translobar**, giving a tissue-like pattern (Figure 1F, 3A-C) and an image **shaped like an anatomical lung** (23,24). The **air-bronchogram** is visualized as **hyperechoic** intraparenchymal images; it is dynamic when moving synchronous with tidal ventilation (25). Its shape can be punctiform or linear/arborescent, with different clinical interpretation (Figure 3A-C – Video 4-6)(26,27).

A diagnostic tool for the acutely ill patient

As for other imaging techniques, lung ultrasound signs are not specific for a diagnosis *per se*. However clinically driven lung ultrasound protocols with focused assessment allow, in particular settings and clinical conditions, to rule in or out quickly and accurately several diagnoses.

Assessment of acute respiratory failure

In the BLUE-protocol, lung ultrasound signs are associated to build up different profiles to be applied in patients presenting to the emergency department with dyspnea (4). **Anterior diffuse lung sliding** with predominant **A-lines** makes the A-profile. The A-profile with

normal posterior fields corresponds to normal parenchyma and orients to non-parenchymal diseases (severe asthma, acute decompensation of chronic obstructive pulmonary disease (COPD)); if associated to ultrasound-detected deep venous thrombosis (DVT) it strongly suggests pulmonary embolism. In a successive study, a combination of A-lines, DVT and subpleural consolidations (corresponding to pulmonary infarctions) allowed the diagnosis of pulmonary embolism with 90% sensitivity and 86% specificity in the emergency department (28).

The A-profile with lobar consolidation in dependent lung regions is associated with pneumonia or the adult respiratory distress syndrome (ARDS)(4).

The presence of A-lines without lung sliding, lung pulse and any B-line strongly suggests pneumothorax, with high sensitivity and moderate context-dependent specificity; the lung point confirms pneumothorax with 100% specificity (4,20,29).

The B-profile is defined by anterior, bilateral, symmetrical B-pattern associated with lung sliding. It may help distinguishing cardiogenic pulmonary edema from acute COPD decompensation and other diseases in the ED (4,9). It is important to underline that a single region with a B-pattern doesn't indicate cardiogenic edema (30). B-pattern distribution helps in differential diagnosis (31): a monolateral B-pattern orients toward pneumonia; if bilateral (i.e. at least two regions per side) it points to cardiogenic pulmonary edema when homogeneous, or to ARDS when non-homogeneous. Assessment of this bilateral and homogeneous B-pattern is now recommended to evaluate and to grade pulmonary edema during heart failure (32,33). Additional ultrasound signs help distinguishing ARDS and cardiogenic edema: ARDS patients have non-homogeneous lung disease combining normal areas with A-lines (spared areas), B-pattern, subpleural and

translobar consolidations, with reduced or abolished lung sliding and irregular and thickened pleural line (Video 3,7, Supplementary Figure 2) (34).

In a different clinical context, patients with a known diffuse parenchymal lung disease (pulmonary fibrosis, sarcoidosis, lymphangitic carcinomatosis, etc) had also a lung ultrasound pattern characterized by diffuse B-lines with irregular and thickened pleura when compared to the healthy population (35).

The C-profile corresponds in the BLUE-protocol to anterior lung consolidations and correlates with pneumonia or ARDS (4). An ultrasound-aided definition of ARDS has also been proposed for the diagnosis in resource-limited settings: in the Kigali modification of the Berlin definition (36), bilateral infiltrates at chest X-ray are replaced by bilateral B-pattern and/or consolidation at lung ultrasound (37).

An ultrasound-based approach can save time in the assessment of dyspnea, but it needs to be integrated with a standard clinical approach to optimize diagnostic accuracy (38).

Finally, a recent single-blind randomized control trial showed that a cardiac, lung and vein ultrasound protocol in patients with acute respiratory failure in the emergency department improves early accurate diagnosis, adequate treatment and better use of advanced diagnostic tests (39).

A comprehensive flow-chart for the assessment of acute respiratory failure based on ultrasound findings is proposed in figure 4.

Assessment of circulatory failure and cardiac arrest

As hypothesized by several authors (40-42) and demonstrated by a prospective observational study (3), an early multiorgan point-of-care ultrasound evaluation allows

reaching almost perfect concordance with final diagnosis of undifferentiated hypotension in the emergency ward. A combined ultrasound assessment of the right ventricle, the inferior vena cava and the lung can rapidly rule out causes of obstructive shock, such as substantial pericardial effusion, acute cor pulmonale or pneumothorax. Left cardiogenic shock can be ruled in or out depending on the presence or absence of a diffuse homogeneous B-pattern. Among the remaining causes of hemodynamic instability, hypovolemic shock is expected to improve after fluid therapy whereas distributive shock has a more variable and transient response. As recently demonstrated, the change from A-lines to B-pattern under fluid therapy early identifies lung extra-vascular leakage in ARDS patients with septic shock and indicates that fluid therapy should be discontinued (43). Accordingly, lung ultrasound can integrate and optimize an ultrasound-aided approach to the septic patient (44).

Echocardiography identifies some of the causes of cardiac arrest (45) and is now recommended (33). The addition of lung, femoral vein and abdomen ultrasound to rule out pneumothorax, DVT and free fluid in the abdomen in cardiac arrest has been proposed (41,46-48). To date, a single prospective application was performed, combining the evaluation of lung sliding to focused echocardiography (5).

A monitoring tool: lung aeration assessment and clinical applications

The number and type of ultrasound artifacts visualized in an intercostal space vary in function of the loss of aeration of the underlying lung regions (8). As shown in vitro (49) and in vivo (50), progressive homogeneous loss of aeration determines the switch from A-

lines to a B-pattern, with a progressively increasing number of B-lines that coalesce more and more. Complete loss of aeration corresponds to tissue-like pattern.

Attempts to semi-quantify loss of aeration have led to different lung ultrasound rating systems (14-16,51,52). The one most frequently used in the ICU distinguishes four steps of progressive loss of aeration (14-16), each corresponding to a score: A-lines or ≤ 2 B-lines (normal aeration – score 0); ≥ 3 well-spaced B-lines (moderate loss of aeration – score 1); coalescent B-lines (severe loss of aeration – score 2); tissue-like pattern (complete loss of aeration – score 3)(Figure 5). This score is computed in six regions per hemithorax: sternum, anterior and posterior axillary lines identify anterior, lateral and posterior areas, each divided into superior and inferior fields (Supplementary Figure 1A). The global lung ultrasound score corresponds to the sum of each region's score and ranges from 0 (all regions are well aerated) to 36 (all regions are consolidated). In ARDS patients, the regional lung ultrasound score is strongly correlated with tissue density assessed with quantitative computed tomography (CT), each step increase of the score from 0 to 3 being associated with a significant gain of density (18). Moreover, the global lung ultrasound score directly correlates both with extra-vascular lung water assessed by transpulmonary thermodilution (53) and with overall lung tissue density assessed by quantitative CT (18).

This score has been successfully employed in different clinical contexts. After a successful spontaneous breathing trial a score higher than 17 is highly predictive of post-extubation distress, while when lower than 13 it is highly predictive of successful weaning (16). An increase in lung ultrasound score is an early warning about the deleterious side effects of fluid resuscitation in septic patients and may guide physicians in fluid administration (43).

Daily lung ultrasound score have been monitored in ARDS patients on veno-venous extracorporeal membrane oxygenation, thus replacing chest X-ray, which is poorly informative in such severely affected lungs (54). A re-aeration score based on the same four patterns can be computed observing the regional changes before and after treatments aimed at improving lung aeration as described in figure 5; it has been successfully applied to rate both antibiotic-induced re-aeration in ventilator-associated pneumonia (VAP) and the increase in lung volume induced by positive end-expiratory pressure (PEEP) in ARDS patients (14,15).

Recent advances suggest that for non-homogeneous diseases, such as ARDS, lung contusion and VAP, the switch from moderate (score 1) to severe (score 2) loss of aeration might be more appropriately identified on the basis of the percentage of the pleural line showing artifacts (55). Moreover, a weakness of current lung ultrasound score is that complete loss of aeration (score 3) is attributed to a lung region whenever a tissue-like pattern is observed, independently of its dimension. This may lead to overestimation of loss of aeration when this pattern involves a small portion of the visualized lung region. To further improve the accuracy of ultrasound assessment of lung aeration, recent findings suggest that a score of 3 should be attributed only to regions where tissue-like pattern is largely predominant (18).

Finally, longitudinal scan – allowing the visualization of the bat sign – is mandatory to correctly identify the pleura within the intercostal space. However, the length of visualized pleura is highly variable among different patients and in the same patient among different intercostal spaces, thus limiting reliability of a score based on number of artifacts per scan

(55). Transversal scan – aligned with the intercostal space – visualized significantly wider and more constant pleural length. Thus, the transversal approach may be preferred when lung ultrasound is performed with the specific aim of a quantitative assessment of lung aeration (18,55).

Lung ultrasound-guided mechanical ventilation

Lung ultrasound was proposed as an imaging tool to guide and monitor mechanical ventilation (56,57). Firstly, it may help airway management: visualizing the oro-tracheal tube beside the trachea, it identifies esophageal intubation and, by visualizing bilateral sliding, it confirms tracheal intubation and excludes selective bronchial positioning (58).

Ultrasound can be used to guide the setting of mechanical ventilation as well. Re-aeration during a recruitment maneuver can be directly and real-time visualized (59). In general, patients with diffuse loss of aeration at ultrasound examination (i.e. also affecting anterior fields) may be PEEP responders while those with focal loss of aeration (i.e. posterior consolidation with normal anterior fields) are more prone to over-distension of the normal parenchyma (15), as previously indicated by CT studies (60). Changes in lung ultrasound score correlated with PEEP-induced increases of end-expiratory lung volume and were therefore proposed for bedside assessment of lung recruitment (15). However, this volume increase does not correspond to the re-inflation of previously collapsed lung tissue (i.e. lung recruitment), as most of the gas enters already inflated lung regions (61). Accordingly, lung ultrasound score parallels lung tissue density and aeration in ARDS patients but

changes of lung ultrasound score are not related with the amount of recruitable lung tissue (18). Whether PEEP-induced changes in size of tissue-like areas could be used to assess lung recruitment at the bedside, although reasonable, still remains to be demonstrated (62).

Patients classified as PEEP non-responders may successfully respond to prone positioning (63). In patients with focal loss of aeration and a normal anterior lung ultrasound pattern, consolidated posterior regions did, in fact, show greater re-aeration with prone positioning than in patients with more diffuse disease (64). Moreover, the amount of re-aeration of posterior lung regions assessed by ultrasound after three hours of prone position was associated with a positive clinical response, defined as a partial pressure of arterial oxygen to fraction of inspired oxygen higher than 300 mmHg after seven days of treatment (Supplementary Figure 1B)(65).

As already stated, the lung ultrasound score can help distinguish patients at high and low risk of post-extubation distress (16). A score 2 pattern seems to best identify the failing patients (66). The lung ultrasound score predicts extubation failure probably because decreased pulmonary aeration is a final common pathway of patients failing extubation for different reasons. The combination of lung ultrasound and other ultrasound techniques in the assessment of the patients to be weaned has been suggested, not only to identify the frailest patients early, but also to understand the underlying mechanism, being the main causes of weaning failure detectable with ultrasound (i.e. unsolved lung disease, diaphragm dysfunction and cardiac failure)(66,67).

Detection and management of respiratory complications in mechanically ventilated patients

Lung ultrasound, thanks to its ready availability at the bedside, could become a key tool for the early diagnosis of the most common complications of mechanical ventilation, such as pleural effusion, alveolar consolidation related to atelectasis or VAP and pneumothorax (56,57).

Pleural effusion appears as a dependent usually echo-free zone acting as an acoustic window (Figure 3D-F)(21,22). Inside the pleural effusion, the lung can be seen as a bright lung line if it remains aerated, or as a floating consolidation if not. Pleural effusion can be easily distinguished from peri-splenic or peri-hepatic fluid collections by the visualization of the diaphragm in longitudinal scan. Lung ultrasound also allows accurate and clinically useful estimates of the volume of effusion (68): in supine position, in transversal scan an interpleural distance of 5 cm or more at the lung base is highly predictive of pleural effusion of 500 mL or more. A linear relationship has also been identified, each centimeter of interpleural distance corresponding to 200 mL of fluid (69). Transudates are always anechoic and homogeneous while exudates may appear echoic, heterogeneous and loculated (Figure 3D-F)(21). Lung ultrasound is also a valid tool to guide effusion drainage and monitor its effectiveness (21,22).

The interposition of gas between the visceral and parietal pleura is marked by the absence of lung sliding, B-lines and lung pulse (7,10,19). Diagnosis of pneumothorax is confirmed by the visualization of a lung point in a more lateral part of the chest wall (20). This corresponds to the limit of the pneumothorax (Figure 2D – Video 2) and can be used to

measure its extension (29): a **lung point beneath the mid-axillary** line in a presumed free collection indicates a **collapse of at least 30%** of the parenchyma. However, in a **completely collapsed** lung **no lung point** can be visualized. Lung ultrasound performs **better than chest X-ray** for diagnosing pneumothorax, particularly in trauma patients (70,71).

In the emergency room lung ultrasound is a valid alternative for early diagnosis of pneumonia in adults (4,26,38,39,72,73). Consolidations have 93% sensitivity and 98% specificity for the diagnosis of community-acquired pneumonia (72). In **ICU patients**, intricate causes of **loss of aeration** may give **rise to B-pattern** and consolidations. Consequently in these patients a **tissue-like pattern is not sufficient for the diagnosis (27)**; instead the presence of a dynamic linear/arborescent **air-bronchogram within a consolidation** seems to be a **specific sign of VAP**. A clinical-ultrasound score can be easily computed at the bedside for **early VAP diagnosis** (27).

Typically, reabsorption atelectasis appears as consolidated parenchyma with a reduced lung volume; the air-bronchogram is either static (initial phase) or completely absent (complete reabsorption of air in small airways)(Figure 3A – Video 4). If the air-bronchogram is dynamic, obstructive atelectasis is ruled out (Video 5,6)(25). No or static air-bronchogram suggests non-patent airway and may be an indication for dis-obstructive fiber-bronchoscopy; a dynamic air-bronchogram corresponds to patent airways and fiber-bronchoscopy may be also indicated to obtain a distal microbiological sample (27).

The vascularization of a lung consolidation can be visualized by color Doppler. A well-perfused lung region with complete loss of aeration corresponds to intrapulmonary shunt, thus suggesting a significant contribution of the consolidation to hypoxemia. However,

color Doppler assessment of lung perfusion is only qualitative; a quantitative assessment may be useful in the future to quantify the intrapulmonary shunt and monitor the response to treatments (74).

Limitations of lung ultrasound

Like other ultrasound techniques, lung ultrasound is operator-dependent and requires training for image acquisition and interpretation. Concerning images acquisition for lung aeration assessment, inter-observer agreement was almost perfect (18); in images interpretation, inter-operator agreement was strong or almost perfect, depending on the scoring system adopted (55). Simple findings can be easily acquired with a short training: anesthesia residents were able to **rule out pneumothorax after 5 minutes of on-line training** (75) and **pleural effusions** were easily detected by ICU **residents after few hours** of theoretical and hands-on work (76). For more advanced skills such as **lung ultrasound score** computation, a longer training with **25 supervised examinations** allowed to reach acceptable concordance between trainees and experts (77). Lung ultrasound is an additional workload for the physician; however, **time required** to perform an extensive examination for lung aeration assessment ranged from 8 minutes for experts **to 10 minutes for trainees** (77).

Lung ultrasound depends on **transmission of ultrasound beams** through the chest wall to the lung surface. This propagation from skin to lung can be **prevented by subcutaneous emphysema** or large **thoracic dressings**. Once the ultrasound beams are transmitted, and

the lung is aerated, the examination only allows analysis of the lung surface. This means that only fields immediately beneath the probe are explored, thus underlying the need for as comprehensive and systematic an examination as possible. Moreover, **caution** is recommended in the **interpretation of lung ultrasound** findings in **diseases** that may have **no or minimal extension** to **peripheral fields** (i.e. deep peribronchial mass/abscess, histiocytosis, tuberculosis, aspergillosis, bronchiectasis).

Finally, **no specific lung ultrasound sign** has been found for the detection of **lung overinflation** (57).

Future perspectives for lung ultrasound

As a monitoring tool, semi-quantitative assessment of lung aeration has greatly developed in the last few years (14-16,51-54). Anyway, a better bedside aeration assessment awaits improvement of the current scoring system with different definitions of moderate and severe loss of aeration (55) and finer quantification of the non-aerated tissue within consolidations (18,62). One additional potential improvement is the detection of overinflation, which is reasonably suggested by reduced sliding (57,78); however, lung sliding has never been objectively quantified and relies on 'eyeball assessment' by expert examiners.

Automation is also being examined, with a view to computing aeration automatically on the basis of the computer-assisted grey-scale analysis (79) or **automatic counting of the B-lines** (80).

Hand-held devices are now available; whether they will improve ultrasound assessment of the critically ill and gradually replace stethoscopes in physicians' pockets is still unclear.

Conclusions

Lung ultrasound is a simple bedside technique with numerous potential translational applications. It may help physicians in the diagnosis of the main respiratory disorders affecting the critically ill, thus suggesting the therapeutic approach in the emergency department and ICU.

Lung ultrasound can be employed to assess and monitor lung aeration in the acute respiratory failure patient and may be a useful tool to guide mechanical ventilation and several procedures, such as recruitment maneuvers, pronation, fiber-bronchoscopy and pleural drainage.

As a consequence, lung ultrasound has generated worldwide enthusiasm among physicians involved in the treatment of critically ill patients. Many clinical applications are nowadays suggested: the extent of their clinical impact and whether lung ultrasound should be part of the basic knowledge of all intensivists will be assessed in the next future.A

Acknowledgments: none

References

1. Zieleskiewicz L, Muller L, Lakhal K, Meresse Z, Arbelot C, Bertrand PM, Bouhemad B, Cholley B, Demory D, Duperret S, Duranteau J, Guervilly C, Hammad E, Ichai C, Jaber S, Langeron O, Lefrant JY, Mahjoub Y, Maury E, Meaudre E, Michel F, Muller M, Nafati C, Perbet S, Quintard H, Riu B, Vigne C, Chaumoitre K, Antonini F, Allaouchiche B, Martin C, Constantin JM, De Backer D, Leone M; CAR'Echo and AzuRea Collaborative Networks. Point-of-care ultrasound in intensive care units: assessment of 1073 procedures in a multicentric, prospective, observational study. *Intensive Care Med* 2015;41(9):1638-47
2. Lamperti M, Bodenham AR, Pittiruti M, Blaivas M, Augoustides JG, Elbarbary M, Pirotte T, Karakitsos D, Ledonne J, Doniger S, Scoppettuolo G, Feller-Kopman D, Schummer W, Biffi R, Desruennes E, Melniker LA, Verghese ST. International evidence-based recommendations on ultrasound-guided vascular access. *Intensive Care Med* 2012;38(7):1105-17
3. Volpicelli G, Lamorte A, Tullio M, Cardinale L, Giraud M, Stefanone V, Boero E, Nazerian P, Pozzi R, Frascisco MF. Point-of-care multiorgan ultrasonography for the evaluation of undifferentiated hypotension in the emergency department. *Intensive Care Med* 2013;39(7):1290-8
4. Lichtenstein DA, Mezière GA. Relevance of lung ultrasound in the diagnosis of acute respiratory failure: the BLUE protocol. *Chest* 2008;134(1):117-25

5. Lien WC, Hsu SH, Chong KM, Sim SS, Wu MC, Chang WT, Fang CC, Ma MH, Chen SC, Chen WJ. US-CAB protocol for ultrasonographic evaluation during cardiopulmonary resuscitation: validation and potential impact. *Resuscitation* 2018;127:125-131
6. Ross AM, Genton E, Holmes JH. Ultrasonic examination of the lung. *J Lab Clin Med* 1968;72(4):556-64
7. Lichtenstein DA, Menu Y. A bedside ultrasound sign ruling out pneumothorax in the critically ill. Lung sliding. *Chest* 1995;108(5):1345-8
8. Lichtenstein D, Mézière G, Biderman P, Gepner A, Barré O. The comet tail artifact. An ultrasound sign of alveolar-interstitial syndrome. *Am J Respir Crit Care Med* 1997;156(5):1640-6
9. Lichtenstein D, Mezière G. A lung ultrasound sign allowing bedside distinction between pulmonary edema and COPD: the comet-tail artifact. *Intensive Care Med* 1998;24:1331-1334
10. Lichtenstein D, Mezière G, Biderman P, Gepner A. The comet-tail artifact, an ultrasound sign ruling out pneumothorax. *Intensive Care Med* 1999;25(4):383-388
11. Xirouchaki N, Kondili E, Prinianakis G, Malliotakis P, Georgopoulos D. Impact of lung ultrasound on clinical decision making in critically ill patients. *Intensive Care Med*. 2014 Jan;40(1):57-65.
12. Brogi E, Bignami E, Sidoti A, Shawar M, Gargani L, Vetrugno L, Volpicelli G, Forfori F. Could the use of bedside lung ultrasound reduce the number of chest x-rays in the intensive care unit? *Cardiovasc Ultrasound* 2017;15(1):23
13. Volpicelli G, Elbarbary M, Blaivas M, Lichtenstein DA, Mathis G, Kirkpatrick AW, Melniker L, Gargani L, Noble VE, Via G, Dean A, Tsung JW, Soldati G, Copetti R,

- Bouhemad B, Reissig A, Agricola E, Rouby JJ, Arbelot C, Liteplo A, Sargsyan A, Silva F, Hoppmann R, Breitzkreutz R, Seibel A, Neri L, Storti E, Petrovic T; International Liaison Committee on Lung Ultrasound (ILC-LUS) for International Consensus Conference on Lung Ultrasound (ICC-LUS). International evidence-based recommendations for point-of-care lung ultrasound. *Intensive Care Med* 2012;38(4):577-91
14. Bouhemad B, Liu ZH, Arbelot C, Zhang M, Ferarri F, Le-Guen M, Girard M, Lu Q, Rouby JJ. Ultrasound assessment of antibiotic-induced pulmonary reaeration in ventilator-associated pneumonia. *Crit Care Med* 2010;38(1):84-92
15. Bouhemad B, Brisson H, Le-Guen M, Arbelot C, Lu Q, Rouby JJ. Bedside ultrasound assessment of positive end-expiratory pressure-induced lung recruitment. *Am J Respir Crit Care Med* 2011;183(3):341-7
16. Soummer A, Perbet S, Brisson H, Arbelot C, Constantin JM, Lu Q, Rouby JJ; Lung Ultrasound Study Group. Ultrasound assessment of lung aeration loss during a successful weaning trial predicts postextubation distress. *Crit Care Med* 2012;40(7):2064-72
17. Lichtenstein DA, Mezière GA, Lagoueyte JF, Biderman P, Goldstein I, Gepner A. A-lines and B-lines: lung ultrasound as a bedside tool for predicting pulmonary artery occlusion pressure in the critically ill. *Chest* 2009; 136(4):1014-1020
18. Chiumello D, Mongodi S, Algieri I, Vergani GL, Orlando A, Via G, Crimella F, Cressoni M, Mojoli F. Assessment of lung aeration and recruitment by CT scan and ultrasound in ARDS patients. *Crit Care Med* 2018, In press

19. Lichtenstein DA, Lascols N, Prin S, Mezière G. The "lung pulse": an early ultrasound sign of complete atelectasis. *Intensive Care Med* 2003;29(12):2187-92
20. Lichtenstein D, Mezière G, Biderman P, Gepner A. The "lung point": an ultrasound sign specific to pneumothorax. *Intensive Care Med* 2000;26(10):1434-40
21. Yu CJ, Yang PC, Chang DB, Luh KT. Diagnostic and therapeutic use of chest sonography: value in critically ill patients. *Am J Roentgenol* 1992;159(4):695-701
22. Lichtenstein D, Hulot JS, Rabiller A, Tostivint I, Meziere G. Feasibility and safety of ultrasound-aided thoracentesis in mechanically ventilated patients. *Intensive Care Med* 1999;25:955-958
23. Yu CJ, Yang PC, Chang DB, Luh KT. Ultrasonographic evaluation of pulmonary consolidation. *Am Rev Respir Dis* 1992;146(3):757-762
24. Lichtenstein DA, Lascols N, Mezière G, Gepner A. Ultrasound diagnosis of alveolar consolidation in the critically ill. *Intensive Care Med* 2004;30(2):276-81
25. Lichtenstein D, Meziere G, Seitz J. The dynamic air bronchogram. A lung ultrasound sign of alveolar consolidation ruling out atelectasis. *Chest* 2009;135:1421-1425
26. Reissig A, Copetti R, Mathis G, Mempel C, Schuler A, Zechner P, Aliberti S, Neumann R, Kroegel C, Hoyer H. Lung ultrasound in the diagnosis and follow-up of community-acquired pneumonia: a prospective, multicenter, diagnostic accuracy study. *Chest* 2012;142(4):965-972
27. Mongodi S, Via G, Girard M, Rouquette I, Misset B, Braschi A, Mojoli F, Bouhemad B. Lung ultrasound for early diagnosis of ventilator-associated pneumonia. *Chest* 2016;149:969-980

28. Nazerian P, Vanni S, Volpicelli G, Gigli C, Zanobetti M, Bartolucci M, Ciavattone A, Lamorte A, Veltri A, Fabbri A, Grifoni S. Accuracy of point-of-care multiorgan ultrasonography for the diagnosis of pulmonary embolism. *Chest* 2014;145(5):950-957.
29. Volpicelli G, Boero E, Sverzellati N, Cardinale L, Busso M, Boccuzzi F, Tullio M, Lamorte A, Stefanone V, Ferrari G, Veltri A, Frascisco MF. Semi-quantification of pneumothorax volume by lung ultrasound. *Intensive Care Med* 2014;40:1460-1467
30. Bataille B, Riu B, Ferre F, Moussot PE, Mari A, Brunel E, Ruiz J, Mora M, Fourcade O, Genestal M, Silva S. Integrated use of bedside lung ultrasound and echocardiography in acute respiratory failure: a prospective observational study in ICU. *Chest* 2014;146(6): 1586–1593
31. Volpicelli G, Caramello V, Cardinale L, Mussa A, Bar F, Frascisco MF. Detection of sonographic B-lines in patients with normal lung or radiographic consolidations. *Med Sci Monit* 2008; 2008:14(3):CR122-8
32. Gheorghide M, Follath F, Ponikowski P, Barsuk JH, Blair JE, Cleland JG, Dickstein K, Drazner MH, Fonarow GC, Jaarsma T, Jondeau G, Sendon JL, Mebazaa A, Metra M, Nieminen M, Pang PS, Seferovic P, Stevenson LW, van Veldhuisen DJ, Zannad F, Anker SD, Rhodes A, McMurray JJ, Filippatos G; European Society of Cardiology; European Society of Intensive Care Medicine. Assessing and grading congestion in acute heart failure: a scientific statement from the acute heart failure committee of the heart failure association of the European Society of Cardiology and endorsed by the European Society of Intensive Care Medicine. *Eur J Heart Fail* 2010;12(5):423-33

33. Lancellotti P, Price S, Edvardsen T, Cosyns B, Neskovic AN, Dulgheru R, Flachskampf FA, Hassager C, Pasquet A, Gargani L, Galderisi M, Cardim N, Haugaa KH, Ancion A, Zamorano JL, Donal E, Bueno H, Habib G. The use of echocardiography in acute cardiovascular care: recommendations of the European Association of Cardiovascular Imaging and the Acute Cardiovascular Care Association. *Eur Heart J Cardiovasc Imaging* 2015 Feb;16(2):119-46
34. Copetti R, Soldati G, Copetti P. Chest sonography: a useful tool to differentiate acute cardiogenic pulmonary edema from acute respiratory distress syndrome. *Cardiovasc Ultrasound* 2008;29;6:16
35. Reissig A, Kroegel C. Transthoracic sonography of diffuse parenchymal lung disease: the role of comet tail artifacts. *J Ultrasound Med* 2003;22(2):173-80
36. ARDS Definition Task Force, Ranieri VM, Rubenfeld GD, Thompson BT, Ferguson ND, Caldwell E, Fan E, Camporota L, Slutsky AS. Acute respiratory distress syndrome: the Berlin Definition. *JAMA* 2012;307(23):2526-33
37. Riviello ED, Kiviri W, Twagirumugabe T, Mueller A, Banner-Goodspeed VM, Officer L, Novack V, Mutumwinka M, Talmor DS, Fowler RA. Hospital Incidence and Outcomes of the Acute Respiratory Distress Syndrome Using the Kigali Modification of the Berlin Definition. *Am J Respir Crit Care Med* 2016;193(1):52-9
38. Zanobetti M, Scorpiniti M, Gigli C, Nazerian P, Vanni S, Innocenti F, Stefanone VT, Savinelli C, Coppa A, Bigiarini S, Caldi F, Tassinari I, Conti A, Grifoni S, Pini R. Point-of-Care Ultrasonography for Evaluation of Acute Dyspnea in the ED. *Chest* 2017;151(6):1295-1301

39. Laursen CB, Sloth E, Lassen AT, Christensen Rd, Lambrechtsen J, Madsen PH, Henriksen DP, Davidsen JR, Rasmussen F. Point-of-care ultrasonography in patients admitted with respiratory symptoms: a single-blind, randomised controlled trial. *Lancet Respir Med* 2014;2(8):638-46
40. Perera P, Mailhot T, Riley D, Mandavia D. The RUSH exam: Rapid Ultrasound in SHock in the evaluation of the critically ill. *Emerg Med Clin North Am* 2010;28(1):29-56
41. Copetti R, Copetti P, Reissig A. Clinical integrated ultrasound of the thorax including causes of shock in nontraumatic critically ill patients. A practical approach. *Ultrasound Med Biol* 2012;38(3):349-59
42. Lichtenstein DA. BLUE-protocol and FALLS-protocol: two applications of lung ultrasound in the critically ill. *Chest* 2015;147(6):1659-1670
43. Caltabeloti F, Monsel A, Arbelot C, Brisson H, Lu Q, Gu WJ, Zhou GJ, Auler JO, Rouby JJ. Early fluid loading in acute respiratory distress syndrome with septic shock deteriorates lung aeration without impairing arterial oxygenation: a lung ultrasound observational study. *Crit Care* 2014;18(3):R91
44. Coen D, Cortellaro F, Pasini S, Tombini V, Vaccaro A, Montalbetti L, Cazzaniga M, Boghi D. Towards a less invasive approach to the early goal-directed treatment of septic shock in the ED. *Am J Emerg Med* 2014;32(6):563-8
45. Breitzkreutz R, Price S, Steiger HV, Seeger FH, Ilper H, Ackermann H, Rudolph M, Uddin S, Weigand MA, Müller E, Walcher F; Emergency Ultrasound Working Group of the Johann Wolfgang Goethe-University Hospital, Frankfurt am Main. Focused

- echocardiographic evaluation in life support and peri-resuscitation of emergency patients: a prospective trial. *Resuscitation* 2010;81(11):1527-33
46. Testa A, Cibinel GA, Portale G, Forte P, Giannuzzi R, Pignataro G, Silveri NG. The proposal of an integrated ultrasonographic approach into the ALS algorithm for cardiac arrest: the PEA protocol. *Eur Rev Med Pharmacol Sci.*2010;14(2):77-88
47. Volpicelli G. Usefulness of emergency ultrasound in nontraumatic cardiac arrest. *Am J Emerg Med* 2011;29(2):216-23
48. Lichtenstein. How can the use of lung ultrasound in cardiac arrest make ultrasound a holistic discipline. The example of the SESAME-protocol. *Med ultrason* 2014; 16(3):252-5
49. Soldati G, Inchingolo R, Smargiassi A, Sher S, Nenna R, Inchingolo CD, Valente S. Ex vivo lung sonography: morphologic-ultrasound relationship. *Ultrasound Med Biol* 2012;38(7):1169-1179
50. Via G, Lichtenstein D, Mojoli F, Rodi G, Neri L, Storti E, Klersy C, Iotti G, Braschi A. Whole lung lavage: a unique model for ultrasound assessment of lung aeration changes. *Intensive Care Med* 2010;36(6):999-1007
51. Baldi G, Gargani L, Abramo A, D'Errico L, Caramella D, Picano E, Giunta F, Forfori F. Lung water assessment by lung ultrasonography in intensive care: a pilot study. *Intensive Care Med* 2013;39:74-84
52. Volpicelli G, Caramello V, Cardinale L, Mussa A, Bar F, Frascisco MF. Bedside ultrasound of the lung for the monitoring of acute decompensated heart failure. *Am J Emerg Med* 2008;26(5):585-91

53. Zhao Z, Jiang L, Xi X, Jiang Q, Zhu B, Wang M, Xing J, Zhang D. Prognostic value of extravascular lung water assessed with lung ultrasound score by chest sonography in patients with acute respiratory distress syndrome. *BMC Pulm Med* 2015;15:98
54. Mongodi S, Pozzi M, Orlando A, Bouhemad B, Stella A, Tavazzi G, Via G, Iotti GA, Mojoli F. Lung ultrasound for daily monitoring of ARDS patients on extracorporeal membrane oxygenation: preliminary experience. *Intensive Care Med* 2018; 44(1):123-4
55. Mongodi S, Bouhemad B, Orlando A, Stella A, Tavazzi G, Via G, Iotti GA, Braschi A, Mojoli F. Modified lung ultrasound score for assessing and monitoring pulmonary aeration. *Ultraschall Med* 2017;38(5):530-537
56. Bouhemad B, Mongodi S, Via G, Rouquette I. Ultrasound for “lung monitoring” of ventilated patients. *Anesthesiology* 2015;122(2):437-47
57. Pesenti A, Musch G, Lichtenstein D, Mojoli F, Amato MBP, Cinnella G, Gattinoni L, Quintel M. Imaging in acute respiratory distress syndrome. *Intensive Care Med* 2016;42(5):686-698
58. Hoffmann B, Gullett JP, Hill HF, Fuller D, Westergaard MC, Hosek WT, Smith JA. Bedside ultrasound of the neck confirms endotracheal tube position in emergency intubations. *Ultraschall Med*. 2014 Oct;35(5):451-8
59. Tusman G, Acosta CM, Constantini M. Ultrasonography for the assessment of lung recruitment maneuvers. *Crit Ultrasound J* 2016;8(1):8
60. Constantin JM, Grasso S, Chanques G, Afort S, Futier E, Sebbane M, Jung B, Gallix B, Bazin JE, Rouby JJ, Jaber S. Lung morphology predicts response to recruitment

- maneuver in patients with acute respiratory distress syndrome. *Crit Care Med* 2010;38(4):1108-17
61. Chiumello D, Marino A, Brioni M, Cigada I, Menga F, Colombo A, Crimella F, Algieri I, Cressoni M, Carlesso E, Gattinoni L. Lung Recruitment Assessed by Respiratory Mechanics and Computed Tomography in Patients with Acute Respiratory Distress Syndrome. What Is the Relationship? *Am J Respir Crit Care Med* 2016;193(11):1254-63
62. Gardelli G, Feletti F, Gamberini E, Bonarelli S, Nanni A, Mughetti M. Using sonography to assess lung recruitment in patients with acute respiratory distress syndrome. *Emerg Radiol* 2009;16(3):219-21
63. Prat G, Guinard S, Bizien N, Nowak E, Tonnelier JM, Alavi Z, Renault A, Boles JM, L'Her E. Can lung ultrasonography predict prone positioning response in acute respiratory distress syndrome patients? *J Crit Care*. 2016 Apr;32:36-41
64. Haddam M, Zieleskiewicz L, Perbet S, Baldovini A, Guervilly C, Arbelot C, Noel A, Vigne C, Hammad E, Antonini F, Lehingue S, Peytel E, Lu Q, Bouhemad B, Golmard JL, Langeron O, Martin C, Muller L, Rouby JJ, Constantin JM, Papazian L, Leone M; CAR'Echo Collaborative Network; AzuRea Collaborative Network. Lung ultrasonography for assessment of oxygenation response to prone position ventilation in ARDS. *Intensive Care Med* 2016;42(10):1546-1556
65. Wang XT, Ding X, Zhang HM, Chen H, Su LX, Liu DW; Chinese Critical Ultrasound Study Group (CCUSG). Lung ultrasound can be used to predict the potential of prone positioning and assess prognosis in patients with acute respiratory distress syndrome. *Crit Care* 2016;30;20(1):385

66. Silva S, Ait Aissa D, Cocquet P, Hoarau L, Ruiz J, Ferre F, Rousset D, Mora M, Mari A, Fourcade O, Riu B, Jaber S, Bataille B. Combined Thoracic Ultrasound Assessment during a Successful Weaning Trial Predicts Postextubation Distress. *Anesthesiology* 2017;127(4):666-674
67. Mongodi S, Via G, Bouhemad B, Storti E, Mojoli F, Braschi A. Usefulness of combined bedside lung ultrasound and echocardiography to assess weaning failure from mechanical ventilation: a suggestive case. *Crit Care Med*. 2013 Aug;41(8):e182-5
68. Vignon P, Chastagner C, Berkane V, Chardac E, Francois B, Normand S, Bonnivard M, Clavel M, Pichon N, Preux PM, Maubon A, Gastinne H. Quantitative assessment of pleural effusion in critically ill patients by means of ultrasonography. *Crit Care Med* 2005; 33: 1757-1763
69. Balik M, Plasil P, Waldauf P, Pazout J, Fric M, Otahal M, Pachel J. Ultrasound estimation of volume of pleural fluid in mechanically ventilated patients. *Intensive Care Med* 2006;32(2):318
70. Blaivas M, Lyon M, Duggal S; A prospective comparison of supine chest radiography and bedside ultrasound for the diagnosis of traumatic pneumothorax. *Acad Emerg Med* (2005); 12:844-849
71. Soldati G, Testa A, Sher S, Pignataro G, La Sala M, Silveri NG. Occult traumatic pneumothorax: diagnostic accuracy of lung ultrasonography in the emergency department. *Chest* 2008;133:204-211
72. Gehmacher O, Mathis G, Kopf A, Scheier M. Ultrasound imaging of pneumonia. *Ultrasound Med Biol* 1995;21(9):1119-1122

73. Cortellaro F, Colombo S, Coen D, Duca PG. Lung ultrasound is an accurate diagnostic tool for the diagnosis of pneumonia in the emergency department. *Emerg Med J* 2012;29(1):19-23
74. Mongodi S, Bouhemad B, Iotti GA, Mojoli F. An ultrasonographic sign of intrapulmonary shunt. *Intensive Care Med* 2016;42(5):912-3
75. Krishnan S, Kuhl T, Ahmed W, Togashi K, Ueda K. Efficacy of an online education program for ultrasound diagnosis of pneumothorax. *Anesthesiology* 2013;118(3):715-21
76. Vignon P, Mücke F, Bellec F, Marin B, Croce J, Brouqui T, Palobart C, Senges P, Truffly C, Wachmann A, Dugard A, Amiel JB. Basic critical care echocardiography: validation of a curriculum dedicated to noncardiologist residents. *Crit Care Med* 2011;39(4):636-42
77. Rouby JJ, Arbelot C, Gao Y, Zhang M, Lv J, An Y, Wang C, Bin D, Barbas CSV, Dexheimer Neto FL, Prior Caltabeloti F, Lima E, Cebey A, Perbet S, Constantin JM; APECHO study group. Training for Lung Ultrasound Score Measurement in Critically Ill Patients. *Am J Respir Crit Care Med* 2018 [Epub ahead of print] doi: 10.1164/rccm.201802-0227LE
78. Markota A, Golub J, Stožer A, Fluher J, Prosen G, Bergauer A, Svenšek F, Sinkovič A. Absence of lung sliding is not a reliable sign of pneumothorax in patients with high positive end-expiratory pressure. *Am J Emerg Med* 2016;34(10):2034-2036
79. Corradi F, Brusasco C, Vezzani A, Santori G, Manca T, Ball L, Nicolini F, Gherli T, Brusasco V. Computer-aided quantitative ultrasonography for detection of

pulmonary edema in mechanically ventilated cardiac surgery patients. *Chest*. 2016 Sep;150(3):640-51

80. Anantrasirichai N, Hayes W, Allinovi M, Bull D, Achim A. Line Detection as an Inverse Problem: Application to Lung Ultrasound Imaging. *IEEE Trans Med Imaging*. 2017 Oct;36(10):2045-2056

Table legends

Table 1: Lung ultrasound signs, patterns and clinical interpretation

(2D: bidimensional ultrasound; PEEP: positive end-expiratory pressure; CT: computed tomography; COPD: chronic obstructive pulmonary disease; ARDS: adult respiratory distress syndrome; VAP: ventilator-associated pneumonia; PV curve: pressure-volume curve; PiCCO: pulse-contour continuous cardiac output; VPLUS: ventilator-associated pneumonia lung ultrasound score).

Figure legends

Figure 1: Basic signs of lung ultrasound. A) The pleural line (white arrow) is identified between the ribs (bat sign); horizontal reverberation artifacts (A-lines – red arrow) at a regular distance indicate a high gas-volume ratio below the parietal pleura (longitudinal scan, linear probe). B) B-lines (*) are vertical artifacts deriving from the pleural line, moving synchronously with lung sliding, usually hyperechoic and laser-shaped, usually reaching the bottom of the screen and erasing A-lines (white arrow: pleural line – longitudinal scan, microconvex probe). C) Subpleural consolidation (dotted red line): an echo-poor image juxtaposed to the pleural line (white arrow) and delimited by irregular boundaries, the “shred sign” (transversal scan, linear probe). D) A very small pleural effusion is visualized as a hypoechoic space between the parietal and visceral pleura (red arrow – longitudinal scan, microconvex probe). E) M-mode of the same scan confirms the presence of the pleural effusion, showing the lung freely floating in it (“sinusoid sign”). F)

Tissue-like pattern identifies lobar consolidation, surrounded by pleural effusion (Lu: Lung; Li: liver – longitudinal scan, phased-array probe).

Figure 2: Basic sign of lung ultrasound in M-mode with corresponding 2D images in longitudinal scan with microconvex probe – red arrows indicate the pleural line. A) M-mode demonstrates normal sliding: above the pleural line, superficial tissues don't move away or toward the probe and are represented as straight lines; the pattern below the pleura is an artifact deriving from it: if the visceral pleura slides, it generates a sandy pattern ("seashore sign"). B) If the visceral pleura doesn't slide but only beats synchronously with the heart, a different M-mode pattern is visualized (lung pulse). C) A pneumothorax is suspected when no lung sliding is visualized, as confirmed by straight lines both above and below the pleural line ("stratosphere sign"). D) Pneumothorax is confirmed by the presence of the lung point, visualized in M-mode as the alternation of "seashore" and "stratosphere" signs, at the location where the collapsed lung comes in touch with the parietal pleura during inspiration (E: expiration; I: inspiration).

Figure 3: A-C) Lobar consolidations are visualized as a tissue-like pattern; the air-bronchograms are visualized as hyperechoic signs within consolidation and provide additional information on consolidation etiology. A) The consolidated lung is visualized in transversal scan; it is homogeneously grey: air-bronchogram is absent which means airway is not clearly patent. Dis-obstructive fiber-bronchoscopy may be indicated; no final conclusions on consolidation etiology can be done. B) Multiple white spots (red arrows) are visualized within the consolidated lung in transversal scan and move synchronously with

tidal ventilation: dynamic air-bronchogram rules out obstructive atelectasis. C) A dynamic linear/arborescent air-bronchogram is specific for community-acquired and ventilator-associated pneumonia (longitudinal scan; dotted red line: diaphragm; S: spleen; L: lung). D-F) Ultrasound features of pleural effusions. D) Pleural effusion is here visualized in transversal scan as an anechoic space between the lung (on the right) and the posterior wall of the chest (on the left); transversal scan allows the measurement of the maximal interpleural distance (red arrow) and the quantification of the fluid collection, providing information about adequacy of chest drainage. Its homogeneous anechoic pattern orients to transudate; the lung appears partially consolidated. E) Septa and adhesions are visualized within the pleural effusion in transversal scan: a flogistic etiology is suggested while septa discourage percutaneous chest drainage. F) A massive echoic pleural effusion is visualized in transversal scan between a collapsed lung (on the right) and the posterior wall of the chest (on the left); the non-homogeneous pattern orients to exudate or blood (depending on clinical context); chest drainage is indicated.

Figure 4: A proposal for a systematic diagnostic approach to acute respiratory failure based on literature findings (DVT: deep venous thrombosis; COPD: chronic pulmonary obstructive disease; ARDS: adult respiratory distress syndrome). #at least 3 B-lines per scan.

Figure 5: Semi-quantification of lung aeration (transversal scans). The aeration score identifies four progressive steps of aeration (score 0: A-lines or ≤ 2 B-lines; score 1: ≥ 3 well-spaced B-lines; score 2: coalescent B-lines; score 3: tissue-like pattern). It is computed in

twelve standard thoracic regions. Re-aeration score may be computed in the same regions to assess lung re-aeration in ventilator-associated pneumonia after antibiotic treatment and in ARDS after PEEP titration. Recent advances suggest to distinguish score 1 and score 2 on the basis of percentage of pleura showing B-lines or subpleural consolidations (less or more than 50%).

Table 1. Lung ultrasound signs, pattern and clinical interpretation

| Signs | Description | Ultrasound interpretation and associated patterns | Clinical conditions and applications | Figures Videos |
|---------------------|---|--|---|--------------------|
| Pleural line | | | | |
| Bat sign | The pleural line is visualized as a horizontal hyperechoic line located in adults 0.5 cm below the rib lines in longitudinal scan in 2D | Correct identification of the pleura within the intercostal space (13) | Particularly useful in clinical conditions potentially compromising the visualization of the pleura (i.e. subcutaneous emphysema, morbid obesity) | Fig. 1A Video 1 |
| Lung sliding | Movement of the pleural line synchronous with tidal ventilation visualized in 2D | Parietal and visceral pleura are in touch and regional ventilation is present | Rules out pneumothorax (sensitivity 95.3%, specificity 91.1%, negative predictive value 100%) (7) | Video 1 |
| | | Reduced sliding | Suggests reduced regional ventilation (hyperinflation (78), emphysematous bullae) | |
| | | Absent sliding | Suggests absent regional ventilation (78) Suggests pneumothorax with context-dependent accuracy (trauma patients: sensitivity 98.1%, specificity 99.2%) (70) | |
| Seashore sign | Straight lines above the pleural line and sandy pattern below the pleural line visualized in M-mode | Confirms the movement of the pleural line synchronous with tidal ventilation, with higher frame rate (4) | Helpful in clinical conditions where sliding is reduced or poorly visible (19) | Fig. 2A |
| Lung pulse | Movement of the pleural line synchronous with heart beats in absence of lung sliding (in 2D or M-mode) | Parietal and visceral pleura are in touch but regional ventilation is impaired | Confirms absence of regional ventilation (obstructed airways, hyperinflation, pleural adherence or bullae) with sensitivity 93.0%, specificity 100% (19) | Fig. 2B |
| | | | Rules out pneumothorax (19) | |
| Stratosphere sign | Straight horizontal lines above and beneath the pleural line in M-mode | Absence of pleural line movement either synchronous with tidal ventilation or with heartbeats. Parietal and visceral pleura may not be in touch (19) | Suggest pneumothorax with context dependent accuracy (trauma patients: sensitivity 98.1%, specificity 99.2%) (70) May be due to high PEEP level (78) | Fig. 2C |
| Lung point | Alternation of normal and abolished sliding during tidal ventilation in 2D; alternation of seashore and stratosphere sign in M-mode | Contact point between the collapsed lung and the pneumothorax air-collection | Confirms pneumothorax (sensitivity 66.0%, specificity 100%) (20) | Fig. 2D Video 2 |

| | | | | |
|---|--|---|--|--------------------|
| | | It's position can be mapped on the thorax Is absent when the lung is completely collapsed | Allows semiquantification of lung collapse: larger than 30% if below mid axillary line (sensitivity 90.9%, specificity 81.3%) (29) | |
| <i>Artifacts</i> | | | | |
| A-lines | | | | |
| Reverberation artifacts visualized as horizontal hyperechoic lines below the pleural line and repeated at a constant distance equal to the distance between pleural line and probe surface – visualized in 2D | High gas-volume ratio below the parietal pleura (18) | | | Fig. 1A Video 1 |
| | A profile: A-lines with maximum 2 B-lines and lung sliding in anterior fields (4) | Corresponds to normal aeration (strong correlation with regional tissue density measured by quantitative CT scan - rs= 0.79) (18) | | |
| | | Rules out pneumothorax (sensitivity 95.3%, specificity 91.1%, negative predictive value 100%) (7) | | |
| | | Allows distinguishing COPD exacerbation from cardiogenic oedema (sensitivity 100%, specificity 92.0%) (9) | | |
| | A-lines with no lung sliding but lung pulse | Confirm absence of regional ventilation (obstructed airways, hyperinflation, pleural adherence or bullae) with sensitivity 93.0%, specificity 100% (19) Rule out pneumothorax (19) | | |
| A-lines with no lung sliding and no lung pulse | Suggest absent regional ventilation (78) Suggest pneumothorax with context-dependent accuracy (trauma patients: sensitivity 98.1%, specificity 99.2% (70) | | | |
| B-lines | | | | |
| Vertical hyperechoic comet-tail artifacts deriving from the pleural line, moving synchronously with it, usually reaching the bottom of the screen in 2D, laser-shaped, erasing the A-lines | A maximum of 2 B-lines per scan can be visualized in healthy lung | Normal lung (4, 18) | | Video 1 |
| | They originate from the visceral pleura | Rule out pneumothorax (sensitivity 100%, specificity 60.0%, negative predictive value 100%) (10) | | |
| | Increased B-lines indicate an increased density of the examined area | Air-tissue ratio is impaired; lung density is increased (strong association with tissue density measured by CT scan R ² =0.62-0.78) (18) | | |
| | B-pattern ("Lung rockets"): ≥3 B-lines per scan are visualized | Indicates interstitial syndrome (17) Allows differential diagnosis between COPD exacerbation and cardiogenic edema (sensitivity 100%, specificity 92.0%) (9) | | Fig. 1B |
| | B-lines distribution allows distinguishing specific diseases (4, 31): | | | |

| | | | |
|--|---|---|--------------------------|
| | <ul style="list-style-type: none"> Focal B-pattern | Depending on the clinical context, it may correspond to pneumonia, atelectasis, lung contusion, pulmonary embolism, pleural disease, neoplasia (4, 31) | |
| | <ul style="list-style-type: none"> Diffuse B-pattern (at least 2 regions per hemithorax): | | |
| | Homogeneous distribution, regular thin pleura, normal sliding and eventual bilateral pleural effusion | Orients to cardiogenic edema (34) | |
| | Non homogeneous distribution, irregular thickened pleura, subpleural and posterior consolidations | Orients to ARDS (34) | Fig. 2 ESM Video 7 |
| | Homogeneous distribution, irregular thickened pleura | Is present in 84.9-100% of cases in diffuse parenchymal lung diseases (fibrosis, sarcoidosis, silicosis...) (35) | |
| | Number and type of B-lines allows quantification of lung aeration by the computation of the lung ultrasound score: | Predicts ARDS mortality (AUC 0.846) (53) and weaning failure (AUC 0.860) (16) | Fig. 2 ESM |
| | <ul style="list-style-type: none"> Substantial agreement between regional lung ultrasound score and quantitative CT classification ($k=0.7$) (18) Strong association between global lung ultrasound score and tissue density measured by CT scan ($R^2=0.62-0.78$) (18) Strong correlation between global lung ultrasound score and EVLW measured by PiCCO ($r^2=0.906$) (53) | Allows monitoring aeration in ECMO patients (54) and fluid resuscitation in ARDS (43) | |
| | | Lung ultrasound reaeration score allows monitoring of VAP response to antibiotics and PEEP induced recruitment as measured by PV curve (correlation with CT $r=0.85$ (14) and $r=0.88$ (15) respectively) | |
| | | Lung ultrasound score variations don't correlate with PEEP induced recruitment as measured by quantitative CT ($R^2=0.01$) (18) | |
| | | Normal anterior fields allow distinguishing pronation responders (sensitivity 58%, specificity 100%, positive predictive value 100%) (63) | |
| <i>Real Images</i> | | | |
| Pleural effusion | | | |
| Dependent and usually echo-free zone acting as an acoustic window between the pleura | Fluid collection (21,22) | | Fig. 3D-F Video 5 |
| | Interpleural distance can be measured | Allows quantification of pleural effusion (depending on the technique: correlation with drained pleural effusion volume 0.51-0.84) (68,69) | Fig. 3D |

| | | | | |
|-----------------------|---|---|--|-------------------------------|
| | | Echotexture can be homogeneous, heterogeneous, loculated | Allows etiologic diagnosis of the effusion (21) Guide the chest drainage (success rate 97%) (21,22) | Fig. 3D-F |
| Sinusoid sign | Sinusoid aspect of visceral pleura movement within the effusion in M-mode | Confirms free fluid collection (22) | Allows distinction of echopoor regions (free effusion, focal collection) (22) | Fig. 1E |
| Consolidations | | | | |
| Shred sign | Subpleural echo-poor images delimited by irregular borders in 2D | Small juxtapleural consolidation | Present in 36.6% of cases in diffuse parenchymal lung diseases (fibrosis, sarcoidosis, interstitial pneumonia, silicosis...) (35) | Fig. 1C Video 3 |
| | | | May corresponds to pulmonary subpleural infarcts in pulmonary embolism (alone: sensitivity 60.9%, specificity 95.9%; combined to vascular and cardiac ultrasound: sensitivity 90.0%, specificity 86.2%) (28) | |
| | | | Supports diagnosis of ventilator-associated pneumonia (alone: sensitivity 81.0%, specificity 41.0%; combined in the VPLUS \geq 2: sensitivity 71.0%, specificity 69.0%) (27) | |
| Tissue like pattern | Homogeneous texture of a lobe, similar to abdominal parenchyma in 2D | Corresponds to complete loss of aeration; a real image is visualized and the lung appears as an anatomical lung | Confirms the diagnosis of community-acquired pneumonia (sensitivity 93.4-99%, specificity 95-97.7%) (26, 73) | Fig. 1F, 3A-C Video 4-6 |
| Air bronchogram | Hyperechoic intraparenchymal images visualized within a tissue like pattern in 2D | It corresponds to air trapped within the consolidation | | |
| | | If absent | Corresponds to complete air reabsorption and potentially not patent airway | Fig. 3A Video 4 |
| | | If static | Correspond to potentially not patent airway – uncomplete air reabsorption Present in 40-90% of pneumonia (25, 72) | |
| | | If dynamic | Corresponds to patent airways: rules out atelectasis (sensitivity 64.0%, specificity 94.0%) (25) Is present in 86.7-97.0% of pneumonia (26, 73) | |
| | | Linear / arborescent | Supports the diagnosis of ventilator-associated pneumonia (alone: sensitivity 44.0%, specificity 81.0%; combined in the VPLUS \geq 2: sensitivity 71.0%, specificity 69.0%) (27) | Fig. 3C Video 6 |

| | | | | |
|--|--|------------|--------------------------------------|--------------------|
| | | Punctiform | Is not specific for a diagnosis (27) | Fig. 3B Video 5 |
|--|--|------------|--------------------------------------|--------------------|

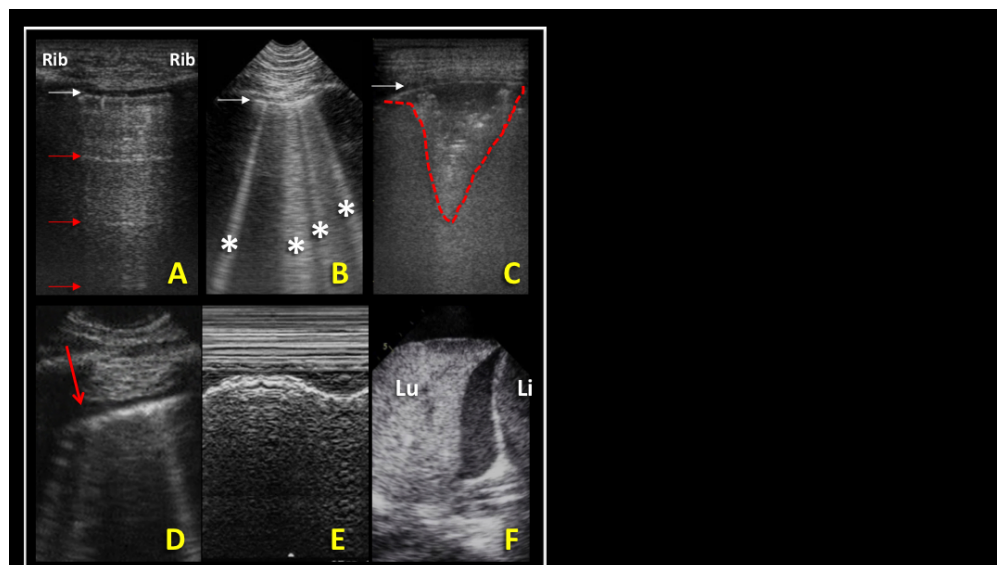


Figure 1: **Basic signs of lung ultrasound.** A) The pleural line (white arrow) is identified between the ribs (bat sign); horizontal reverberation artifacts (A-lines – red arrow) at a regular distance indicate a high gas-volume ratio below the parietal pleura (longitudinal scan, linear probe). B) B-lines (*) are vertical artifacts deriving from the pleural line, moving synchronously with lung sliding, usually hyperechoic and laser-shaped, reaching the bottom of the screen and erasing A-lines (white arrow: pleural line – longitudinal scan, microconvex probe). C) Subpleural consolidation (dotted red line): an echo-poor image juxtaposed to the pleural line (white arrow) and delimited by irregular boundaries, the “shred sign” (transversal scan, linear probe). D) A very small pleural effusion is visualized as a hypoechoic space between the parietal and visceral pleura (red arrow – longitudinal scan, microconvex probe). E) M-mode of the same scan confirms the presence of the pleural effusion, showing the lung freely floating in it (“sinusoid sign”). F) Tissue-like pattern identifies lobar consolidation, surrounded by pleural effusion (Lu: Lung; Li: liver – longitudinal scan, phased-array probe).

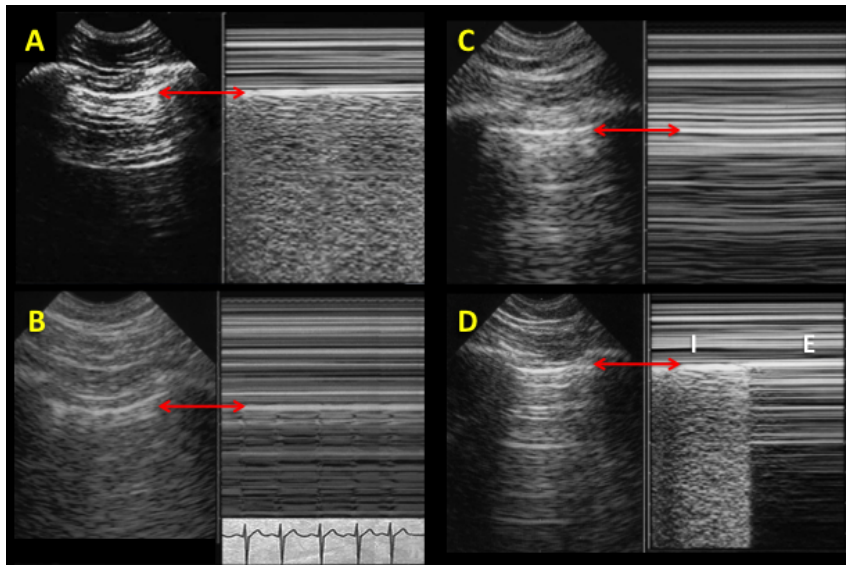


Figure 2: Basic sign of lung ultrasound in M-mode with corresponding 2D images in longitudinal scan with microconvex probe – red arrows indicate the pleural line. A) M-mode demonstrates normal sliding: above the pleural line, superficial tissues don't move away or toward the probe and are represented as straight lines; the pattern below the pleura is an artifact deriving from it: if the visceral pleura slides, it generates a sandy pattern ("seashore sign"). B) If the visceral pleura doesn't slide but only beats synchronously with the heart, a different M-mode pattern is visualized (lung pulse). C) A pneumothorax is suspected when no lung sliding is visualized, as confirmed by straight lines both above and below the pleural line ("stratosphere sign"). D) Pneumothorax is confirmed by the presence of the lung point, visualized in M-mode as the alternation of "seashore" and "stratosphere" signs, at the location where the collapsed lung comes in touch with the parietal pleura during inspiration (E: expiration; I: inspiration).

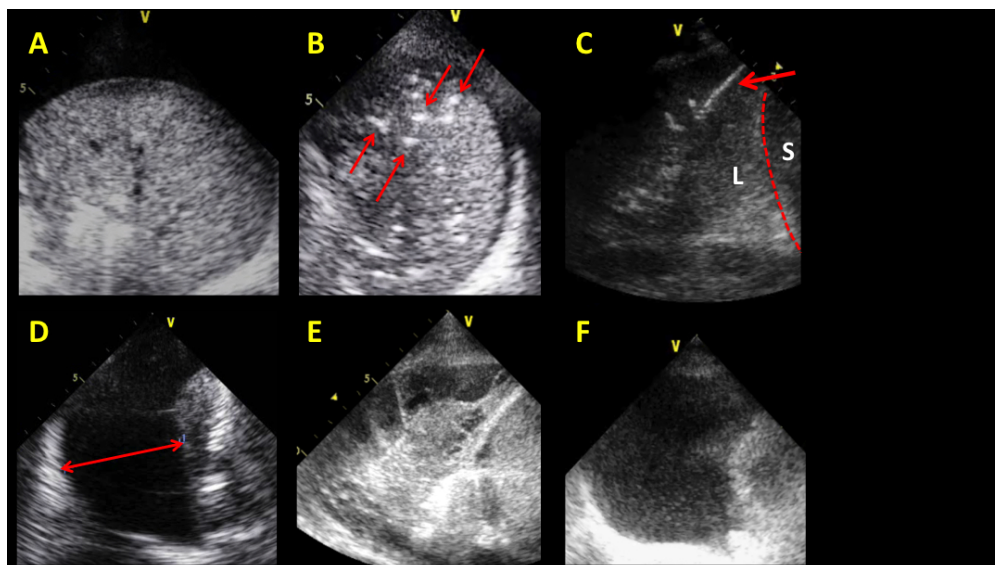


Figure 3: A-C) Lobar consolidations are visualized as a tissue-like pattern; the air-bronchograms are visualized as hyperechoic signs within consolidation and provide additional information on consolidation etiology. A) The consolidated lung is visualized in transversal scan; it is homogeneously grey; air-bronchogram is absent which means airway is not clearly patent. Dis-obstructive fiber-bronchoscopy may be indicated; no final conclusions on consolidation etiology can be done. B) Multiple white spots (red arrows) are visualized within the consolidated lung in transversal scan and move synchronously with tidal ventilation: dynamic air-bronchogram rules out obstructive atelectasis. C) A dynamic linear/arborescent air-bronchogram is specific for community-acquired and ventilator-associated pneumonia (longitudinal scan; dotted red line: diaphragm: S: spleen; L: lung). D-F) Ultrasound features of pleural effusions. D) Pleural effusion is here visualized in transversal scan as an anechoic space between the lung (on the right) and the posterior wall of the chest (on the left); transversal scan allows the measurement of the maximal interpleural distance (red arrow) and the quantification of the fluid collection, providing information about adequacy of chest drainage. Its homogeneous anechoic pattern orients to transudate; the lung appears partially consolidated. E) Septa and adhesions are visualized within the pleural effusion in transversal scan: a flogistic etiology is suggested while septa discourage percutaneous chest drainage. F) A massive echoic pleural effusion is visualized in transversal scan between a collapsed lung (on the right) and the posterior wall of the chest (on the left); the non-homogeneous pattern orients to exudate or blood (depending on clinical context); chest drainage is indicated.

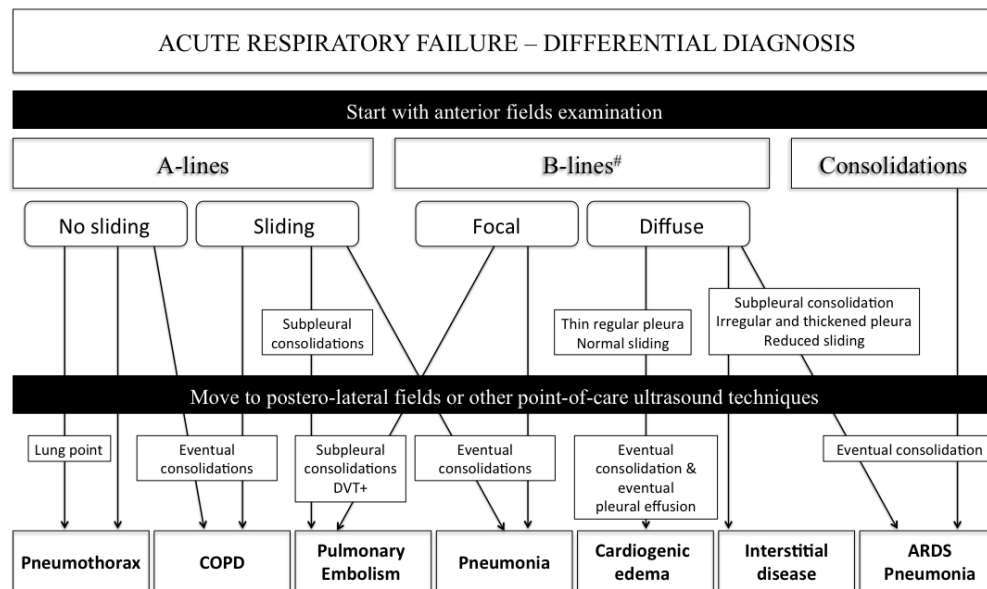


Figure 4: A **proposal for a systematic diagnostic approach to acute respiratory failure** based on literature findings (DVT: deep venous thrombosis; COPD: chronic pulmonary obstructive disease; ARDS: adult respiratory distress syndrome). #at least 3 B-lines per scan.

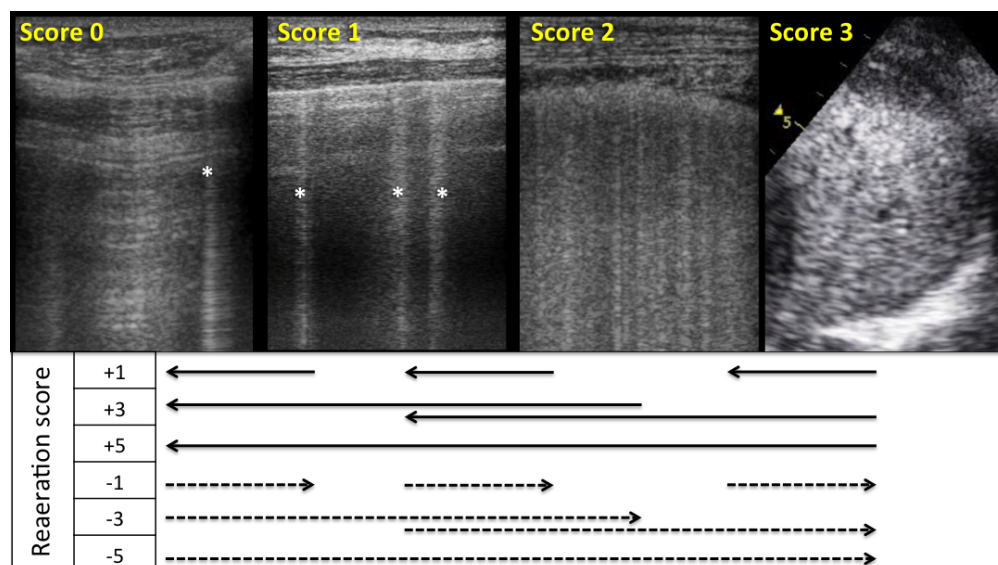


Figure 5: Semi-quantification of lung aeration (transversal scans). The aeration score identifies four progressive steps of aeration (score 0: A-lines or ≤ 2 B-lines; score 1 ≥ 3 well-spaced B-lines; score 2: coalescent B-lines; score 3: tissue-like pattern). It is computed in twelve standard thoracic regions. Re-aeration score may be computed in the same regions to assess lung re-aeration in ventilator-associated pneumonia after antibiotic treatment and to identify PEEP responders. Recent advances suggest to distinguish score 1 and score 2 on the basis of percentage of pleura showing B-lines or subpleural consolidations (less or more than 50%).

Supplementary Legends

Supplementary Figure 1: Identification of the thoracic areas in different systematic approaches to lung ultrasound. A) Anterior, lateral and posterior areas are identified on each hemithorax by sternum, anterior and posterior axillary lines, corresponding to the three ultrasound areas of the BLUE protocol (4); each area can be further divided in superior and inferior regions. A simplified examination focused on regions 1-4 per hemithorax is recommended in emergency department (13). A 6-region per hemithorax approach is commonly used for semi-quantification of lung aeration in intensive care unit (14-16, 18, 55). B) A focused examination of posterior areas has been proposed for the assessment of prone position effects on lung aeration (65).

Supplementary Figure 2: Ultrasound features of ARDS patients (transversal scans). A) An area with severe loss of aeration and coalescent B-lines (white arrow) is visualized close to a normally aerated area (spared area – red dotted arrow). B) Lung sliding is abolished and lung pulse is frequently remarked in anterior fields (M-mode; white arrow: pleural line). C) The pleura is thickened and irregular (red arrow). D) Posterior consolidations are almost constant. E) Subpleural consolidations are frequent; they correspond to echo-poor regions hanged on the pleura and moving with it, delimited by irregular boundaries.

Video Legends

Video 1: Normal pattern: the pleural line is visualized within the bat sign; it moves synchronous with tidal ventilation (lung sliding). Multiple A-lines are visualized at a regular distance. Longitudinal scan; linear probe.

Video 2: No pleural movement (no lung sliding, no lung pulse) is visualized in expiration; during inspiration, a lung sliding appears from the right of the screen: this corresponds to the lung point and is specific for pneumothorax. Transversal scan; linear probe.

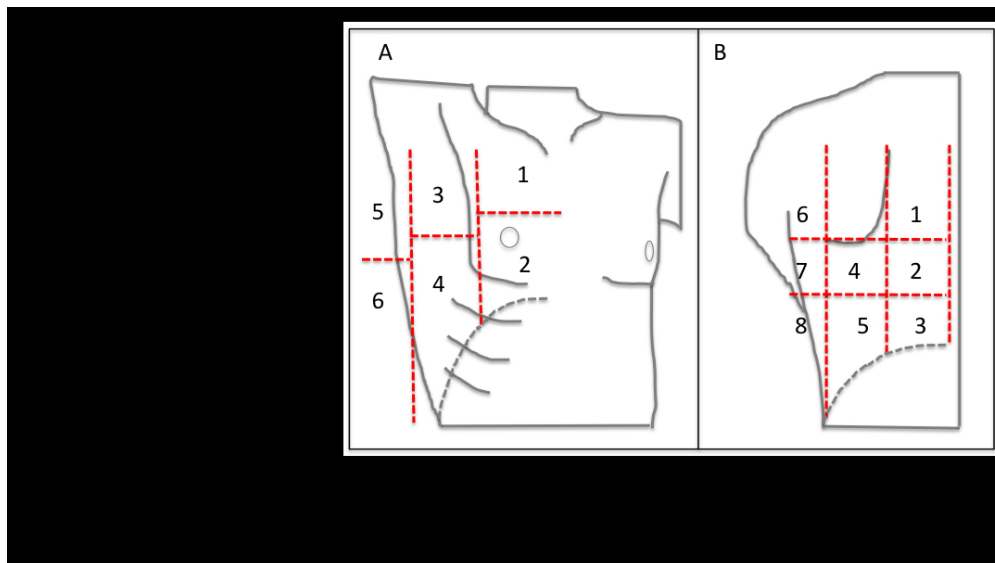
Video 3: Subpleural consolidations are echo-poor images hanging on the pleura and moving synchronous with it. Transversal scan; linear probe.

Video 4: A tissue-like pattern is visualized, corresponding to lung consolidation; it's homogeneously grey, with no air-bronchogram; it suggests obstructive atelectasis. Transversal scan; phased-array probe.

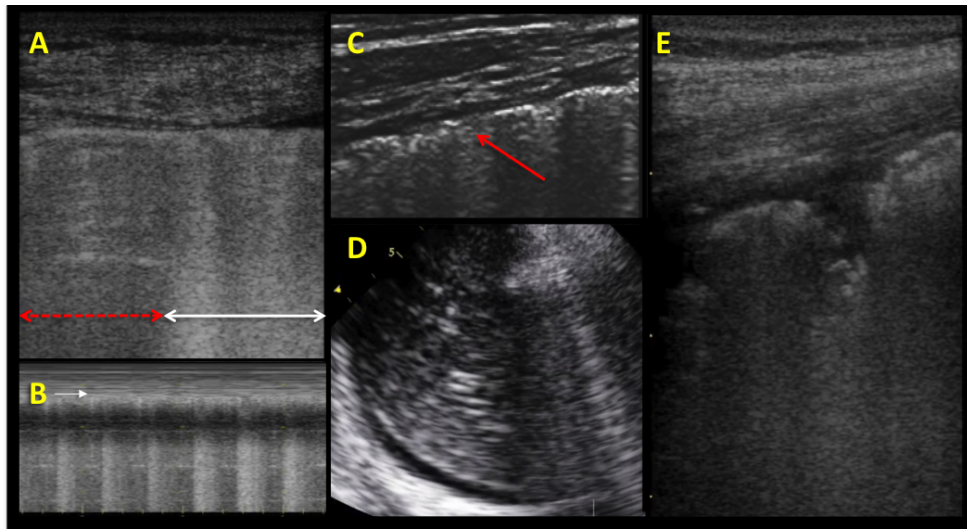
Video 5: A tissue-like pattern is visualized, corresponding to lung consolidation; in inspiration, a dynamic punctiform air-bronchogram appears and rules out obstructive atelectasis. A pleural effusion surrounds the consolidation. Transversal scan; phased-array probe.

Video 6: A tissue-like pattern is visualized, corresponding to lung consolidation. A linear dynamic air-bronchogram is visualized, thus orienting to ventilator-associated pneumonia in this ICU patient. The diaphragmatic dome separates the lung from the spleen. Longitudinal scan; phased-array probe.

Video 7: In ARDS, a normally aerated pattern with A-lines (spared area) is frequently visualized close to areas with severe loss of aeration (coalescent B-lines and subpleural consolidations). Transversal scan; linear probe.



Supplementary Figure 1: **Identification of the thoracic areas in different systematic approaches** to lung ultrasound. A) Anterior, lateral and posterior areas are identified on each hemithorax by sternum, anterior and posterior axillary lines, corresponding to the three ultrasound areas of the blue protocol (4); each area can be further divided in superior and inferior regions. A simplified examination focused on regions 1-4 per hemithorax is recommended in emergency department (13). A 6 regions per hemithorax approach is commonly used for semi-quantification of lung aeration in intensive care unit (14-16, 18, 55). B) A focused examination of posterior areas has been proposed for the assessment of prone position effects on lung aeration (65).



Supplementary Figure 2: Ultrasound features of ARDS patients (transversal scans). A) An area with severe loss of aeration and coalescent B-lines (white arrow) is visualized close to a normally aerated area (spared area – red dotted arrow). B) Lung sliding is abolished and lung pulse is frequently remarked in anterior fields (M-mode; white arrow: pleural line). C) The pleura is thickened and irregular (red arrow). D) Posterior consolidations are almost constant. E) Subpleural consolidations are frequent; they correspond to echo-poor regions hanged on the pleura and moving with it, delimited by irregular boundaries.